

STABILITY ANALYSIS OF A NONLINEAR COUPLED-CORE  
REACTOR CONTROL SYSTEM

Tain-Sou Tsay  
Institute of Electronics,  
National Chiao-Tung  
University, Taiwan, R.O.C.

and Kuang-Wei Han  
Chung-Shan Institute and adjunct  
professor at National Chiao-  
Tung University, Taiwan, R.O.C.

ABSTRACT-In this paper, stability-equation method is applied to the analysis of a large coupled-core reactor control system having multiple nonlinearities and adjustable parameters. The characteristics of the limit-cycle and the asymptotically stable regions can be easily defined in a parameter plane. A numerical example is given and comparisons with other methods in current literature are made.

### I. INTRODUCTION

In current literature, several methods have been applied to the analysis of large coupled-core reactor control systems[1-3]. Raju and Stone[1] have derived an analytical model and investigated system stability using the describing function approach; Raju and Josselson[2] have obtained conditions of stability using the Popov criterion; Tsouri and Rootenberg[3] have applied the Tsytkin locus method for limit cycle and stability analysis.

In the above mentioned methods, all the systems are considered symmetrical, and it is assumed that each system can be reduced into two single-input, single-output systems [1,3], then the single-output systems are analyzed. In this paper, a general method based upon the stability-equation method[4,5] is proposed. The considered systems need not be symmetrical and reduced. In addition, the systems may have both nonlinearities and adjustable parameters. The main approach of the proposed method is to analyze system stability and the existence of limit cycles by finding the simultaneous solutions of both the stability-equations[4,5] and the harmonic-balance equations[6-13].

### II. AN ANALYTICAL MODEL OF THE COUPLED-CORE REACTOR

The linearized equations of the coupled-core reactor control system considered in this paper are as follows[1-3]:

$$\dot{n}_1 = -\frac{D}{A}n_1 + \frac{D}{A}n_2 - \frac{b}{A}n_1 + \frac{rh}{A}T_1 + \frac{h}{A}P_1 \quad (1-a)$$

$$\dot{n}_2 = -\frac{D}{A}n_2 + \frac{D}{A}n_1 - \frac{b}{A}n_2 + \frac{rh}{A}T_2 + \frac{h}{A}P_2 \quad (1-b)$$

$$\dot{c}_1 = \frac{b}{A}n_1 - \lambda c_1 \quad (1-c)$$

$$\dot{c}_2 = \frac{b}{A}n_2 - \lambda c_2 \quad (1-d)$$

$$T_1 = Kn_1 - aT_1 \quad (1-e)$$

$$T_2 = Kn_2 - aT_2 \quad (1-f)$$

where:

- $n_1, n_2$  -deviations of power in core#1 and core#2, respectively, and  $n$  is taken as proportional to neutron flux.
- $c_1, c_2$  -deviations in average concentration of delayed neutrons in core#1 and in core#2, respectively.
- $T_1, T_2$  -deviations in temperature for core#1 and core#2, respectively.
- $K$  -proportionality constant between power and temperature.
- $D$  -power coupling coefficient between cores.
- $\lambda$  -effective delayed neutron decay-time constant.
- $b$  -fraction of neutrons delayed.
- $A$  -prompt neutron generation time.
- $r$  -reactivity-temperature coefficient.
- $a$  -heat removal coefficient.
- $h$  -steady-state power level.
- $p$  -reactivity.

Taking the Laplace transformation of Eq.(1), the block diagram of the model including the controller[1-3] is shown in Fig.1(a), where

$$G_1(S) = G_2(S) = \frac{h}{AS(1+T_m S)} \quad (2-a)$$

$$G_{11}(S) = G_{22}(S) = \frac{(S+a)(S+\lambda)}{(S+\frac{D}{A})(S+\lambda)(S+a) + \frac{b}{A}S(S+a) + \frac{rKh}{A}(S+\lambda)} \quad (2-b)$$

$$G_{12}(S) = G_{21}(S) = \frac{D}{A} \quad (2-c)$$

$T_m$  is the time constant of the control-rod drive motor;  $N_1$  and  $N_2$  represent the on-off

\*Manuscript is first received by IEEE namely May 28, 1987.

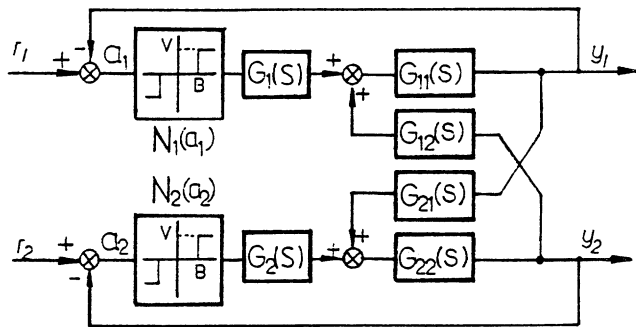


Fig.1(a). Block diagram of the control system for a large coupled-core reactor.

relays. The equivalent system block diagram of Fig.1(a) is shown in Fig.1(b), where

$$W_{11}(S) = G_1(S)G_{11}(S) / \Delta(S) \quad (3-a)$$

$$W_{21}(S) = G_1(S)G_{11}(S)G_{21}(S)G_{22}(S) / \Delta(S) \quad (3-b)$$

$$W_{12}(S) = G_2(S)G_{11}(S)G_{12}(S)G_{22}(S) / \Delta(S) \quad (3-c)$$

$$W_{22}(S) = G_2(S)G_{22}(S) / \Delta(S) \quad (3-d)$$

and  $\Delta(S) = 1 - G_{11}(S)G_{21}(S)G_{21}(S)G_{22}(S)$ .

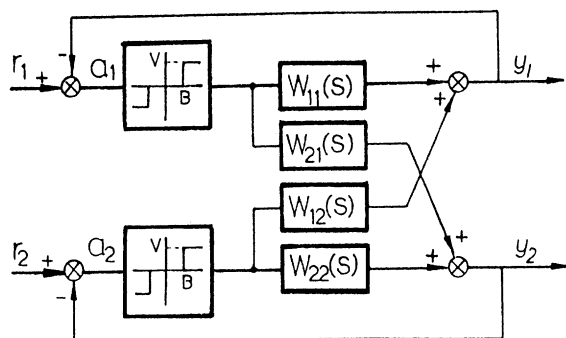


Fig.1(b). Equivalent block diagram of the system shown in Fig.1(a).

### III. THE BASIC APPROACH

Consider the system shown in Fig.1(b). Assume that the input signals to the nonlinearities  $N_1$  and  $N_2$  are

$$a_1 = A_1 \exp[j(\omega t + \theta_1)] \quad (4-a)$$

and

$$a_2 = A_2 \exp[j(\omega t + \theta_2)] \quad (4-b)$$

respectively, where  $A_1$  and  $A_2$  are the amplitudes;  $\theta_1$  and  $\theta_2$  are the phase angles. Consider  $a_1$  as the reference signal; i.e., to

let  $\theta_1$  to be zero, then the harmonic-balance equations [6-13] of loop-1 and loop-2 are

$$A_1 N_1(a_1) W_{11}(j\omega) + A_2 e^{j\theta_2} N_2(a_2) W_{12}(j\omega) = -A_1 \quad (5-a)$$

and

$$A_1 N_1(a_1) W_{21}(j\omega) + A_2 e^{j\theta_2} N_2(a_2) W_{22}(j\omega) = -A_2 e^{j\theta_2} \quad (5-b)$$

respectively, where  $\theta_2$  is the phase angle of the input signal to the nonlinearity  $N_2$  with  $a_1$  as the reference signal;  $N_1(a_1)$  and  $N_2(a_2)$  are the describing functions (or equivalent gains [14,15]) of the nonlinearities  $N_1$  and  $N_2$ , respectively.

From Eq.(5-a), one has

$$e^{j\theta_2} = - \frac{A_1 [1 + N_1(a_1) W_{11}(j\omega)]}{A_2 N_2(a_2) W_{12}(j\omega)} \quad (6)$$

Similarly, Eq.(5-b) gives

$$e^{j\theta_2} = - \frac{N_1(a_1) W_{21}(j\omega)}{A_2 [1 + N_2(a_2) W_{22}(j\omega)]} \quad (7)$$

Equating Eqs.(6) and (7), one has

$$F(j\omega) = 1 + N_1(a_1) W_{11}(j\omega) + N_2(a_2) W_{22}(j\omega) + N_1(a_1) N_2(a_2) [W_{11}(j\omega) W_{22}(j\omega) - W_{12}(j\omega) W_{21}(j\omega)] = 0 \quad (8)$$

which is the characteristic equation of the considered system. Note that  $N_1(a_1)$  and  $N_2(a_2)$  are considered as varying parameters.

Since  $N_1$  and  $N_2$  are two single-valued nonlinearities [1,2], Eq.(8) can be decomposed into two stability-equations [4,5] as

$$F_e(\omega) = B_1(\omega) + N_1(a_1) C_1(\omega) + N_2(a_2) D_1(\omega) + N_1(a_1) N_2(a_2) E_2(\omega) = 0 \quad (9)$$

and

$$F_o(\omega) = B_2(\omega) + N_1(a_1) C_2(\omega) + N_2(a_2) D_2(\omega) + N_1(a_1) N_2(a_2) E_2(\omega) = 0 \quad (10)$$

From Eqs.(9), one has

$$N_2(a_2) = - \frac{B_1(\omega) + N_1(a_1) C_1(\omega)}{D_1(\omega) + N_1(a_1) E_1(\omega)} \quad (11)$$

Similarly, Eq.(10) gives

$$N_2(a_2) = - \frac{B_2(\omega) + N_1(a_1) C_2(\omega)}{D_2(\omega) + N_1(a_1) E_2(\omega)}, \quad (12)$$

Equating Eqs.(11) and (12), one has

$$[C_1(\omega)E_2(\omega) - C_2(\omega)E_1(\omega)]N_1(a_1)^2 + [C_2(\omega)D_1(\omega) + B_2(\omega)E_1(\omega) - C_1(\omega)D_2(\omega) - B_1(\omega)E_2(\omega)] \times N_1(a_1) + [B_2(\omega)D_1(\omega) - B_1(\omega)D_2(\omega)] = 0 \quad (13)$$

For specified values of frequency( $\omega$ ), the values of  $N_1(a_1)$  can be found by solving Eq.(13), then the corresponding values of  $N_2(a_2)$  can be found from Eq.(11) or Eq.(12).

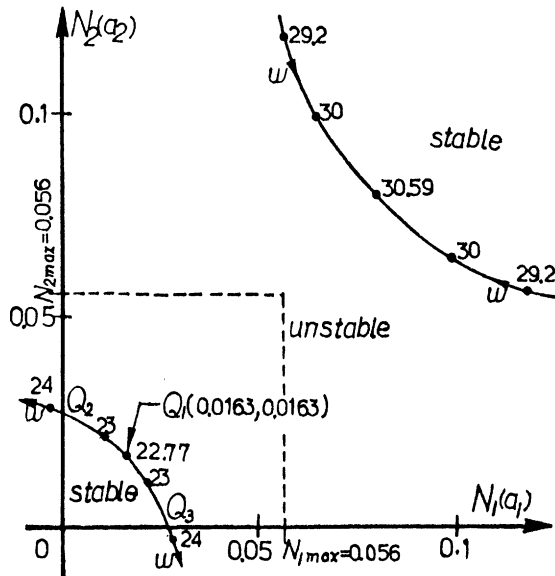


Fig.2. Root-loci of the stability-equations for Case 1 with M=22.

For a number of suitable values of  $\omega$ , the real solutions (roots) of  $N_1(a_1)$  and  $N_2(a_2)$  can be plotted in a  $N_1(a_1)$  vs.  $N_2(a_2)$  plane. The typical root loci for a latter case are shown in Fig.2.

By use of Fig.2, the conditions of having a limit cycle are explained as follows:

(i) Every point on the curves as shown in Fig.2 represents a set of  $N_1(a_1)$ ,  $N_2(a_2)$  and  $\omega$  which can satisfy the condition that a limit cycle may exist if the roots  $\omega_{ei}$  and  $\omega_{oj}$  of the even and odd stability-equations  $F_{ei}(\omega)$  and  $F_{oj}(\omega)$ , respectively, are all real and alternating in sequence. There is an exception, however, when one root pair is equal to the other (i.e.,  $\omega_{ei} = \omega_{oj} = \omega$ ) [4,5]. But unfortunately for nonlinear multivariable systems, there are infinite number of solutions which can satisfy this condition [13]. This is quite different from that of the single-input, single-output systems.

(ii) If the root-loci shown in Fig.2 separate the stable and unstable regions, then a limit cycle may exist. The reason is that, if the system becomes stable (unstable) when the amplitudes  $A_1$  and  $A_2$  increase (decrease), a stable limit cycle may exist at the stability boundary [4,5,16].

(iii) A limit cycle may exist only if the corresponding values of  $N_1(a_1)$  and  $N_2(a_2)$  of the root-loci are less than the maximal gains

( $N_{1max}$  and  $N_{2max}$ ) of the nonlinearities. For example, in Fig.2 only the section between points  $Q_2$  and  $Q_3$  can give a limit cycle.

(iv) A limit cycle may exist only if the roots  $N_1(a_1)$  and  $N_2(a_2)$  satisfy both Eqs.(5-a) and (5-b). From Eqs.(5-a) and (5-b), the possible simultaneous solution can be found by equating the real and imaginary parts of Eqs.(6) and (7), respectively; i.e.,

$$\begin{vmatrix} e^{j\theta_{26}} & -e^{j\theta_{27}} \end{vmatrix} = 0 \quad (14)$$

where  $\theta_{26}$  and  $\theta_{27}$  represent the phase angles found from Eqs.(6) and (7), respectively.

If the considered nonlinear system can satisfy all the above four conditions, a limit cycle may exist. The three parameters  $A_1$ ,  $A_2$  and  $\omega$  of the limit cycle are defined by Eqs.(9), (10) and (14). Additional explanations are given in the following section.

#### IV. ANALYSIS OF THE CONTROL SYSTEM

CASE 1: Assume that the numerical values of the parameters of the system considered are at  $b=.0064, A=.1, \lambda=.001 \text{sec}, K=10 \text{ F/MW.sec}, a=10/\text{sec}, r=.001/\text{F}, h=40 \text{MW}, D=.015, B=.25 \text{MW}, T=.07 \text{sec},$  and  $V=M \times 10^{-3} \delta k/k.\text{sec}$  [3]. For  $M=22$  and for a number of frequencies ( $\omega$ ), the simultaneous solutions of Eqs.(9) and (10) are shown in Fig.2 where the stability of each region has been checked. At every point on the root loci, it has been checked that the roots  $\omega_{ei}$  and  $\omega_{oj}$  of the stability-equations  $F_{ei}(\omega)$  and  $F_{oj}(\omega)$ , respectively, are all real and alternating in sequence except that one root pair is equal to the other (i.e.,  $\omega_{ei} = \omega_{oj} = \omega$ ).

By inspecting the root-loci shown in Fig.2, the section between points  $Q_2$  and  $Q_3$  can satisfy Conditions (i) to (iii). Solving Eq.(14) along the section between points  $Q_2$  and  $Q_3$ , the point  $Q(0.0163, 0.0163)$  with oscillating frequency  $\omega=22.77 \text{ rad/sec}$  and amplitudes  $A_1=A_2=1.703$  can satisfy condition (iv). Therefore, a limit cycle may exist at point  $Q_1$ . This fact is supported by checking the roots  $\omega_{ei}$  and  $\omega_{oj}$  of the stability-equations in the neighborhood of point  $Q_1$  [16]. Fig.3 shows the  $\omega_{ei}$  and  $\omega_{oj}$  loci for  $N_1(a_1)$  is fixed at  $0.0163$  (i.e.,  $A_1=1.703$ ) while  $N_2(a_2)$  is varying. From Fig.3(a), one can see that if the value of  $N_2(a_2)$  is less than  $0.0163$  (i.e.,  $A_2=1.703$ ), the roots  $\omega_{ei}$  and  $\omega_{oj}$  are alternative in sequence, then the corresponding system is stable [4,5,16]. If the value of  $N_2(a_2)$  is larger than  $0.0163$ , the corresponding system is unstable. A similar result can be obtained when  $N_2(a_2)$  is fixed at  $0.0163$  (i.e.,  $A_2=1.703$ ) and  $N_1(a_1)$  is varying. Therefore, a stable limit cycle will exist at the stability boundary where  $N_2(a_2)=0.0163$ ; i.e.,  $A_2=1.703$ .

In Fig.2, for another branch of the root-loci, the corresponding values of  $N_1(a_1)$  and  $N_2(a_2)$  are larger than the maximal gains of  $N_1(a_1)$  and  $N_2(a_2)$ , respectively; therefore, no limit cycle can exist.

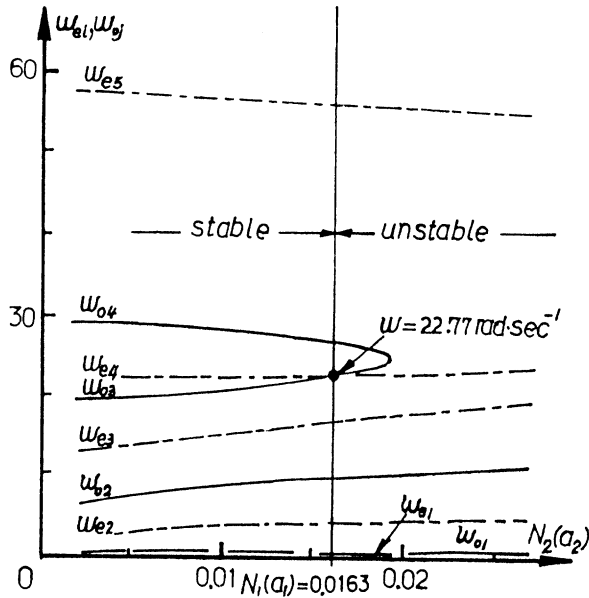


Fig. 3. Root-loci of  $\omega_{ei}$  and  $\omega_{oj}$  of the stability-equations with fixed  $N_1(a_1)$  and varying  $N_2(a_2)$ .

Note that the root-loci can also be plotted in the  $A_1$  vs.  $A_2$  plane by solving Eqs. (11), (12) and (13) which  $N_1(a_1)$  and  $N_2(a_2)$  directly relate to the describing functions of the nonlinearities  $N_1$  and  $N_2$ ; i.e.,

$$N_i(a_i) = \frac{4V}{\pi A_i} \left(1 - \frac{B^2}{A_i^2}\right)^{1/2} \quad i=1,2 \quad (15)$$

The result is given in Fig. 4 where point  $Q_4$  represents a stable limit cycle. In this case condition (iii) is not necessary for analysis.

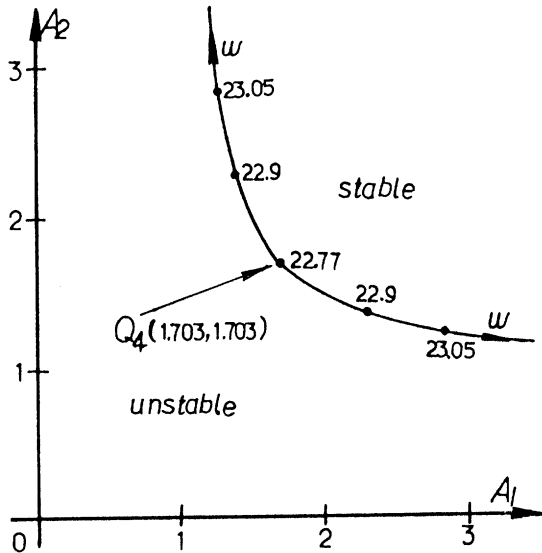


Fig. 4. Root-loci of the stability-equations for Case 1 with  $M=22$ .

By computer simulation, Fig. 5 shows the limit cycle of the system for  $M=22$ . The

simulated result is quite close to that obtained by calculation.

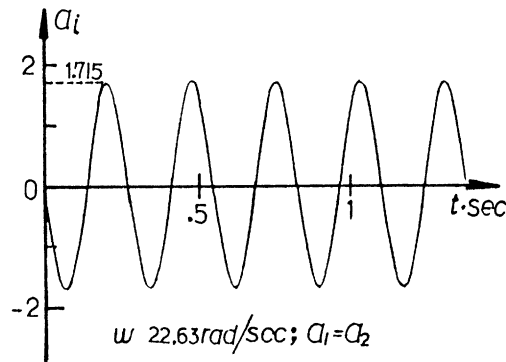


Fig. 5. The simulated limit-cycle of Case 1 for  $M=22$ .

CASE 2: For the system considered in Case 1, assume that the nonlinearities  $N_1$  and  $N_2$  are replaced by two double-valued nonlinearities [3] as shown in Fig. 6. Then the descri-

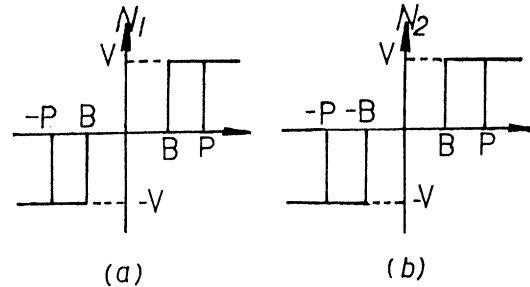


Fig. 6. Nonlinearities of Case 2.

bing functions  $N_1(a_1)$  and  $N_2(a_2)$  of Eqs. (5) - (8) are replaced by

$$N_k(a_k) = N_{kr}(a_k) + jN_{ki}(a_k) \quad k=1,2 \quad (16)$$

$$\text{where } N_{kr} = \frac{2V}{\pi A_k} \left[ \left(1 - \frac{B^2}{A_k^2}\right)^{1/2} + \left(1 - \frac{P^2}{A_k^2}\right)^{1/2} \right]$$

$$N_{ki} = -\frac{2V(P-B)}{\pi A_k^2}, \quad A_k \geq B.$$

By using the same approach as in Case 1, Eq. (8) is decomposed into

$$\begin{aligned} F_e(\omega) = & B_1(\omega) + N_{1r}(a_1)C_1(\omega) - N_{1i}(a_1)C_2(\omega) \\ & + N_{2r}(a_2)D_1(\omega) - N_{2i}(a_2)D_2(\omega) \\ & + [N_{1r}(a_1)N_{2r}(a_2) - N_{1i}(a_1)N_{2i}(a_2)] \times \\ & E_1(\omega) - [N_{1r}(a_1)N_{2i}(a_2) + N_{1i}(a_1) \times \\ & N_{2r}(a_2)] E_2(\omega) = 0 \end{aligned} \quad (17)$$

and

$$\begin{aligned} F_o(\omega) = & B_2(\omega) + N_{1r}(a_1)C_2(\omega) + N_{1i}(a_1)C_1(\omega) \\ & + N_{2r}(a_2)D_2(\omega) + N_{2i}(a_2)D_1(\omega) + [N_{1r}(a_1) \times \end{aligned}$$

$$\begin{aligned}
& N_{2r}(a_2) - N_{1i}(a_1)N_{2i}(a_2) \} E_2(\omega) \\
& + [N_{1r}(a_1)N_{2i}(a_2) + N_{1i}(a_1)x \\
& N_{2r}(a_2)] E_1(\omega) = 0 \quad (18)
\end{aligned}$$

where  $B_i(\omega)$ ,  $C_i(\omega)$ ,  $D_i(\omega)$  and  $E_i(\omega)$  are the same as those of Eqs.(9) and (10). For  $M=22$ ,  $B=0.15\text{MW}$  and  $P=0.25\text{MW}$ , and for a number of frequencies( $\omega$ ), the root locus of the stability-equations is plotted as shown in Fig.7. It has been checked that every point on this root-locus can satisfy conditions (i) and (ii). Solving Eq.(14) along this root-locus, the point  $Q_5(1.752, 1.752)$  with an oscillating frequency  $\omega=22.526$  rad/sec represents a stable limit cycle.

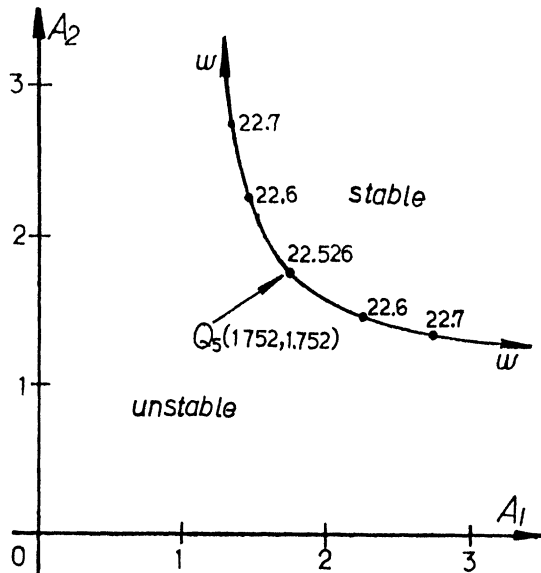


Fig.7. Root-loci of stability-equations for Case 2 with  $M=22$ ,  $B=.15\text{MW}$  and  $P=.25\text{MW}$ .

By computer simulation, the limit cycle is shown in Fig.8, which is quite close to that obtained by calculation.

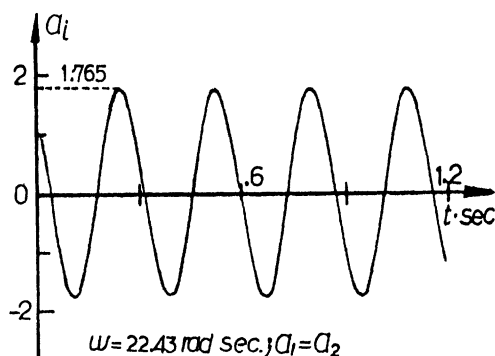


Fig.8. The simulated limit-cycle of Case 2 for  $M=22$ ,  $B=0.15\text{MW}$  and  $P=0.25\text{MW}$ .

Note that, although Eqs.(17) and (18) are more complex than Eqs.(9) and (10), the approach is straightforward and the computations can be easily made on a computer.

## V. CONSIDERATION OF PARAMETER ADJUSTMENT

In this section, control systems with adjustable parameters are considered. Assume that two adjustable parameters  $K_1$  and  $K_2$  are cascaded by the nonlinearities  $N_1$  and  $N_2$ , respectively, then Eqs.(5-a) and (5-b) become

$$k_1 A_1 N_1(a_1) W_{11}(j\omega) + k_1 A_2 e^{j\theta_2} N_2(a_2) W_{12}(j\omega) = -A_1 \quad (19-a)$$

and

$$k_2 A_1 N_1(a_1) W_{21}(j\omega) + k_2 A_2 e^{j\theta_2} N_2(a_2) W_{22}(j\omega) = -A_2 e^{j\theta_2} \quad (19-b)$$

respectively. Eq.(19-a) gives

$$e^{j\theta_2} = - \frac{A_1 [1 + k_1 N_1(a_1) W_{11}(j\omega)]}{k_1 A_2 N_2(a_2) W_{12}(j\omega)} \quad (20)$$

Similarly, Eq.(19-b) gives

$$e^{j\theta_2} = - \frac{k_2 N_1(a_1) W_{21}(j\omega)}{A_2 [1 + k_2 N_2(a_2) W_{22}(j\omega)]} \quad (21)$$

Equating Eqs.(20) and (21), one has

$$\begin{aligned}
F(j\omega) = & 1 + k_1 N_1(a_1) W_{11}(j\omega) + k_2 N_2(a_2) W_{22}(j\omega) \\
& + k_1 k_2 N_1(a_1) N_2(a_2) [W_{11}(j\omega) W_{22}(j\omega) \\
& - W_{12}(j\omega) W_{21}(j\omega)] = 0 \quad (22)
\end{aligned}$$

which is the characteristic equation of the system under consideration. The stability-equations are

$$\begin{aligned}
F_e(\omega) = & B_1(\omega) + k_1 [N_{1r}(a_1) C_1(\omega) - N_{1i}(a_1) C_2(\omega)] \\
& + k_2 [N_{2r}(a_2) D_1(\omega) - N_{2i}(a_2) D_2(\omega)] \\
& + k_1 k_2 \{ [N_{1r}(a_1) N_{2r}(a_2) - N_{1i}(a_1) x \\
& N_{2i}(a_2)] E_1(\omega) - [N_{1r}(a_1) N_{2i}(a_2) \\
& + N_{1i}(a_1) N_{2r}(a_2)] \} E_2(\omega) = 0 \quad (23)
\end{aligned}$$

and

$$\begin{aligned}
F_o(\omega) = & B_2(\omega) + k_1 [N_{1r}(a_1) C_2(\omega) + N_{1i}(a_1) C_1(\omega)] \\
& + k_2 [N_{2r}(a_2) D_2(\omega) + N_{2i}(a_2) D_1(\omega)] \\
& + k_1 k_2 \{ [N_{1r}(a_1) N_{2r}(a_2) - N_{1i}(a_1) x \\
& N_{2i}(a_2)] E_2(\omega) + [N_{1r}(a_1) N_{2i}(a_2) \\
& + N_{1i}(a_1) N_{2r}(a_2)] E_1(\omega) = 0 \quad (24)
\end{aligned}$$

where  $B_i(\omega)$ ,  $C_i(\omega)$ ,  $D_i(\omega)$  and  $E_i(\omega)$  are the same as those in Eqs.(9) and (10). The condition defined in Eq.(14), now, becomes

$$\left| e^{j\theta_{220}} - e^{j\theta_{221}} \right| = 0 \quad (25)$$

where  $\theta_{220}$  and  $\theta_{221}$  represent the phase angles found by Eqs.(20) and (21), respectively. The desirable solutions are  $A_1$ ,  $A_2$ ,  $K_1$ ,  $K_2$ , and  $\omega$ . Thus for specified values of  $A_1$  and  $\omega$ , one can find the solutions  $A_2$ ,  $k_1$  and  $k_2$  by use of Eqs.(23)-(25). Now, for a specified value of  $A_1$  and a number of values of  $\omega$ , a limit-cycle locus can be plotted in a  $K_1$  vs.  $K_2$  plane. For a number of constant- $A_1$  limit-cycle loci, the limit-cycle region and the asymptotically stable region can be found in the  $K_1$  vs.  $K_2$  plane[16]. Similarly, one can plot the constant- $A_2$  limit-cycle loci in the  $K_1$  vs.  $K_2$  plane for specified values of  $A_2$  and a number of values of  $\omega$ .

Case 3: Consider the system in Case 2. Assume that two adjustable parameters  $K_1$  and  $K_2$  are cascaded by nonlinearities  $N_1$  and  $N_2$  as shown in Fig.6, respectively. For  $M=22$ ,  $B=0.15MW$  and  $P=0.25MW$ , following the above presented procedure the limit-cycle loci are plotted as shown in Fig.9, where

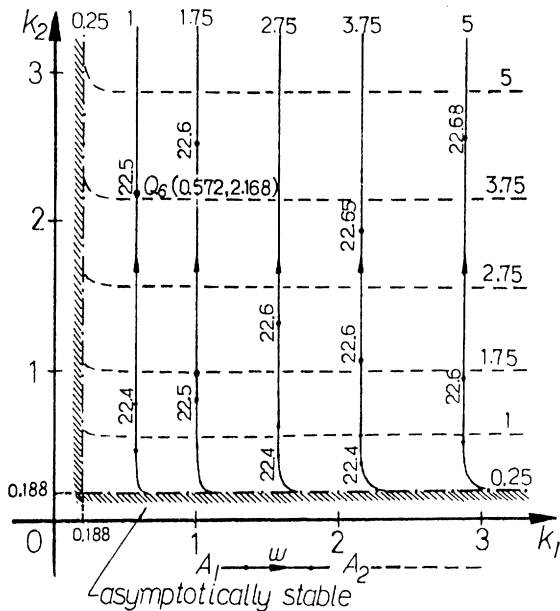


Fig.9. Limit-cycle loci of Case 3 for  $M=22$ ,  $B=0.15MW$  and  $P=0.25MW$ .

the solid lines and dash lines are the constant- $A_1$  and the constant- $A_2$  limit-cycle loci, respectively; the shaded region shows the asymptotically stable region[16]. For illustration, the limit cycle represented by point  $Q_6(0.5718, 2.1683)$ , with amplitudes  $A_1=1$ ,  $A_2=3.788$ , and with oscillating frequency  $\omega=22.5rad/sec$ , has been simulated; the result is shown in Fig.10.

CASE 4: Consider the system in Case 2. Assume that the nonlinearities  $N_1$  and  $N_2$  as

shown in Fig.6 are followed by two adjustable parameters  $K_1$  and  $K_2$ , respectively. This is

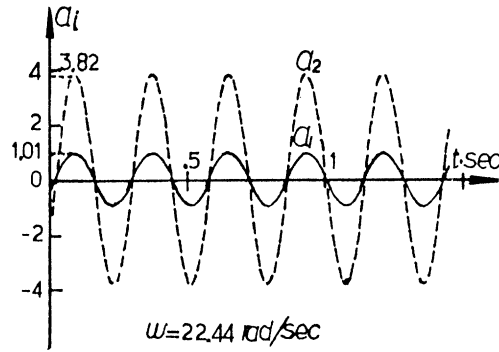


Fig.10. The simulated limit-cycle of Case 3 with  $K_1=0.5718$  and  $K_2=2.6183$ .

equivalent to the case that the amplitudes of the nonlinearities  $N_1$  and  $N_2$  are adjustable. The harmonic-balance equations of the system are found as

$$k_1 A_1 N_1(a_1) W_{11}(j\omega) + k_2 A_2 e^{j\theta_2} N_2(a_2) W_{12}(j\omega) = -A_1 \quad (26-a)$$

and

$$k_1 A_1 N_1(a_1) W_{21}(j\omega) + k_2 A_2 e^{j\theta_2} N_2(a_2) W_{22}(j\omega) = -A_2 e^{j\theta_2} \quad (26-b)$$

Following the same procedure as indicated by Eqs.(22) to (25), the constant- $A_1$  limit-cycle loci are plotted as shown in Fig.11, where the shaded region is the asymptotically stable region.

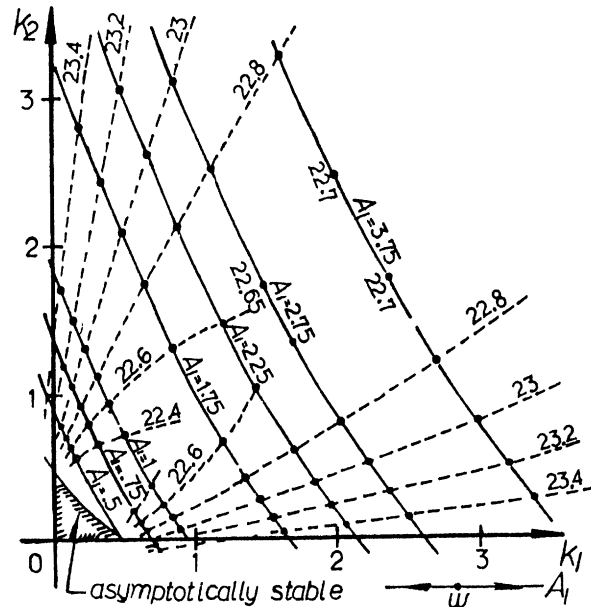


Fig.11. Limit-cycle loci of Case 4 for  $M=22$ ,  $B=0.15MW$  and  $P=0.25MW$ .

Table 1 shows the calculated and simulated results of some points in Fig.11. It can be

Parameters		Calculated			Simulated		
$k_1$	$k_2$	$\omega$	$A_1$	$A_2$	$\omega$	$A_1$	$A_2$
0.3142	0.6555	22.4	0.75	0.9329	22.29	0.752	0.941
0.5729	0.1848	22.4	0.75	0.542	22.33	0.756	0.547
0.4958	0.7106	22.4	1.00	1.1147	22.32	1.008	1.124
0.6810	0.3715	22.4	1.00	0.8343	22.28	1.008	0.842
0.8364	1.3206	22.6	1.75	2.0051	22.46	1.768	2.017
1.6226	0.03463	23.4	1.75	0.934	23.27	1.771	0.972
2.0296	0.8124	22.8	2.75	2.115	22.77	2.777	2.143

Table 1. Calculated and simulated results of Case 4.

seen that the simulated results are quite close to those of calculated.

From Figs.9 and 11, one can see that the minimal values of  $K_1$  and  $K_2$  which give rise to a limit cycle are at  $K_1=K_2=0.188$  for the symmetrical case[3]. Then the critical value of  $M$  for having a limit cycle is  $M_c=K_1 X_M=0.188 \times 22=4.1$ , which is quite close to the result found by Tsouri and Rootenberg using the Tsytkin Locus Method[3].

Note that if the nonlinearities and the linear transfer functions are not symmetrical (such as  $K_1 \neq K_2$ ) the proposed method can be applied in the same way as for the symmetrical case. It is also worthwhile to point out that, by use of the asymptotically stable region, the limit cycle can be eliminated by adjusting the parameters in the system.

## VI. CONCLUSIONS

In this paper, the stability-equation method has been applied for limit cycle analysis of a nonlinear coupled-core reactor control system. The proposed method is simpler than the other methods in current literature, and it has the potential to be applied to very complicated, nonlinear, symmetrical and asymmetrical systems.

## REFERENCES

- G. V. S. Raju and R. S. Stone, "Control System in Spatially Large Cores," IEEE Trans. on Nuclear Science, Vol. NS-17, No.1, pp.534-540, Feb. 1970.
- G. V. S. Raju and R. Josselson, "Stability of Reactor Control System in Coupled Core Reactors," IEEE Trans. on Nuclear Science, Vol. NS-18, No.1, pp.388-394, Feb. 1971.
- N. Tsouri, J. Rootenberg and L. J. Lidofsky, "Stability Analysis of a Reactor Control System by the Tsytkin Locus Method," IEEE Trans. on Nuclear Science, Vol. NS-20, No.1, pp.649-660, Feb. 1973.
- K. W. Kan and G. J. Thaler, "High Order System Analysis and Design using the Root Locus Method," J. of Franklin Institute, Vol.281, No.2, pp.99-133, Feb. 1966.
- K. W. Han, "Nonlinear Control System: Some Practical Method," Academic Culture Company, 1977.
- D. P. Atherton, "Nonlinear Control Engineering," Van Nostrand Reinhold, London, 1975.
- A. I. Mees, "Describing Functions, Circle Criteria and Multiloop Feedback Systems," PROC. IEE, Vol.120, No.1, pp.126-130, 1973.
- N. Ramani and D. P. Atherton, "Frequency Response Method for Nonlinear Multivariable Systems," Canadian Conference on Automatic Control, University of New Brunswick, Fredericton, 1973.
- S. Shankar and D. P. Atherton, "Graphical Stability Analysis of Nonlinear Multivariable Control Systems," Int. J. Control, Vol.25, pp.375-388, 1977.
- A. K. El Shakkany and D. P. Atherton, "Computer Graphics Method for Nonlinear Multivariable Systems," IFAC Computer-Aided Design of Control Systems, pp.157-161, 1979.
- J. O. Gray and P. M. Taylor, "Frequency Responses Method in the Design of Multivariable Nonlinear Feedback Systems," 4-th IFAC, Multivariable Technological Systems, pp.225-232, 1977.
- J. O. Gray and P. M. Taylor, "Computer Aided Design of Multivariable Nonlinear Control Systems using Frequency Domain Techniques," Automatica, Vol.15, pp.281-297, 1979.
- J. O. Gray and N. B. Nakhla, "Prediction of Limit Cycle in Multivariable Nonlinear Systems," PROC. IEE, Vol.128, Pt.D, No.5, pp.283-241, Sept. 1981.
- R. G. Cameron and M. Tabatabai, "Prediction the Existence of Limit Cycles using Walsh Function: some Further Results," Int. J. System Sci. Vol.14, No.9, pp.1043-1064, 1983.
- B. Kouvaritakis and R. G. Cameron, "The Use of Walsh Functions in Multivariable Limit Cycle Prediction," Automatica, Vol.19, No.5, pp.513-522, 1983.
- T. S. Tsay and K. W. Han, "Analysis of a Nonlinear Sampled-data Proportional Navigation System having Adjustable Parameters," J. of Franklin Institute, Vol.321, No.4, pp.203-218, April 1986.